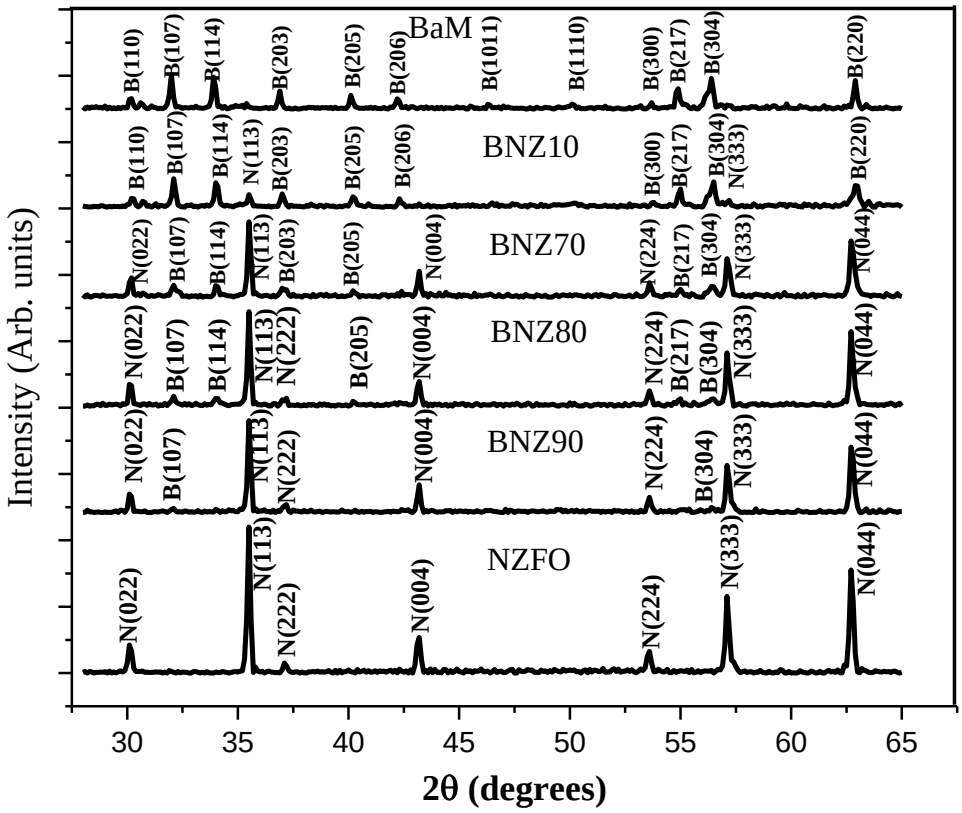


Figure S-1: *X-ray diffraction (XRD) patterns for magnetic composites with (100-x) wt.% barium hexaferrite (BaM) and x wt.% of nickel-zinc ferrite (NZFO) for a series of x-values. The indexed reflections correspond to the hexagonal BaM (indicated by B) and cubic spinel NZFO (indicated by N) phases.*

Table S-1: The NZFO and BaM contents of the BNZ composites estimated from X-ray diffraction data in Figure 1 and Figure S-1.

Sample code	NZFO content (percentage)	BaM content (percentage)
BNZ10	9.8	90.2
BNZ20	14.3	85.7
BNZ30	33.7	66.3
BNZ40	38.9	61.1
BNZ50	49.3	50.7
BNZ60	56.6	43.4
BNZ70	75.0	25.0
BNZ80	80.5	19.5
BNZ90	4.9	95.1

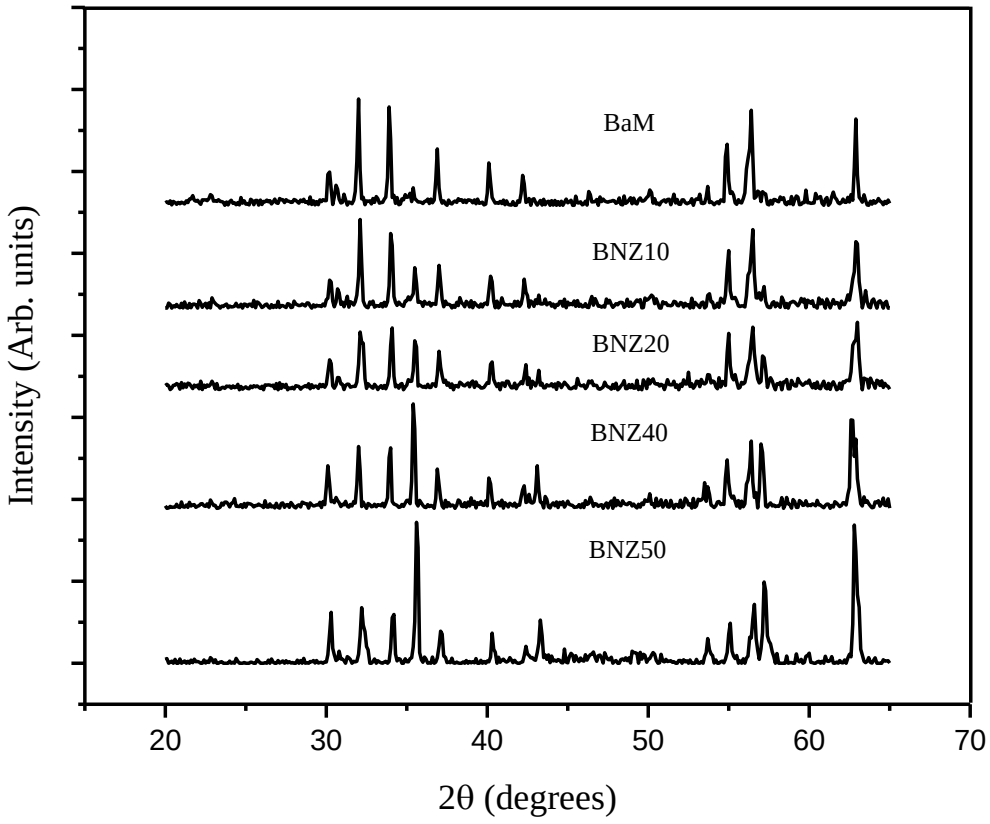


Figure S-2: . *X-ray diffraction (XRD) patterns for platelets of the BNZx composites with (100-x) wt.% barium hexaferrite (BaM) and x wt.% of nickel-zinc ferrite (NZFO) for a series of x-values. The patterns for 2θ = 20-65 deg were obtained specifically to verify the phase purity of the composites, since the presence of an impurity phase, $BaFe_2O_4$, will have the most intense diffraction peaks in the 20 to 30 deg. region. The data indicate the absence or too small an amount of the impurity that cannot be detected by XRD.*

Table S-2: Chemical composition of BaM and NZFO in BNZx composites determined by EDS/EDAX. The results are for different SEM magnifications and surface spots on the composite platelets.

Sample	Spectrum#	Composition	Comments
BNZ-40	1	$Ni_{0.72}Zn_{0.28}Fe_2O_4$ $BaFe_{14.5}O_{19}$	1000x
	2	$Ni_{1.0}ZnFe_2O_4$ $BaFe_{11.53}O_{19}$	1000x
	3	$Ni_{0.67}Zn_{0.33}Fe_2O_4$ $BaFe_{10.1}O_{19}$	1000x
	4	$Ni_{0.68}Zn_{0.32}Fe_2O_4$ $BaFe_{14.2}O_{19}$	5000x
	5	$Ni_{0.81}Zn_{0.19}Fe_2O_4$ $BaFe_{43.95}O_{19}$	5000x
	6	$Ni_{0.75}Zn_{0.25}Fe_2O_4$ $BaFe_{10.1}O_{19}$	5000x
	7	$Ni_{0.72}Zn_{0.28}Fe_2O_4$ $BaFe_{10.1}O_{19}$	5000x
BNZ-60	1	$Ni_{0.79}Zn_{0.21}Fe_{1.0}O_4$ $Ni_{1.18}Zn_{0.31}Fe_{1.5}O_4$ *	1000x, 10kV
	2	$Ni_{0.8}Zn_{0.2}Fe_1O_4$ $BaFe_{10.1}O_{19}$	
	3	$Ni_{0.24}Zn_{0.76}Fe_{2.0}O_4$ $BaFe_{6.8}O_{19}$	15kV, 2500x
	4	$BaFe_{12}O_{19}$	15kV, 2500x
	5	$Ni_{1.0}Zn_0Fe_{2.77}O_4$ $BaFe_{12}O_{19}$	15kV, 1000x
	6	NZFO=0 $BaFe_{12}O_{19}$	15kV, 2500x
	7	$Ni_{0.82}Zn_{0.18}Fe_2O_4$ $BaFe_{11.05}O_{19}$	15kV, 1000x
	8	$Ni_{0.85}Zn_{0.15}Fe_2O_4$ $BaFe_{10.4}O_{19}$	15kV, 1000x
	9	$Ni_{0.78}Zn_{0.22}Fe_2O_4$ $BaFe_{12.28}O_{19}$	15kV, 1000x

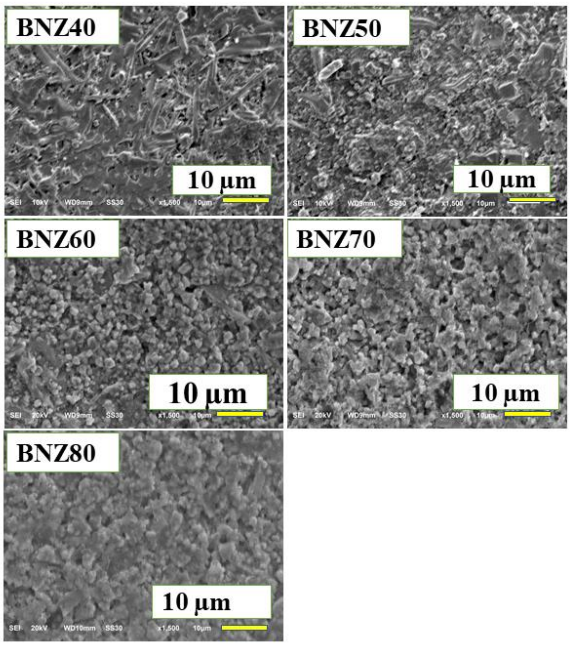


Figure S-3: SEM images for BNZ40, BNZ50, BNZ60, BNZ70 and BNZ80 composites

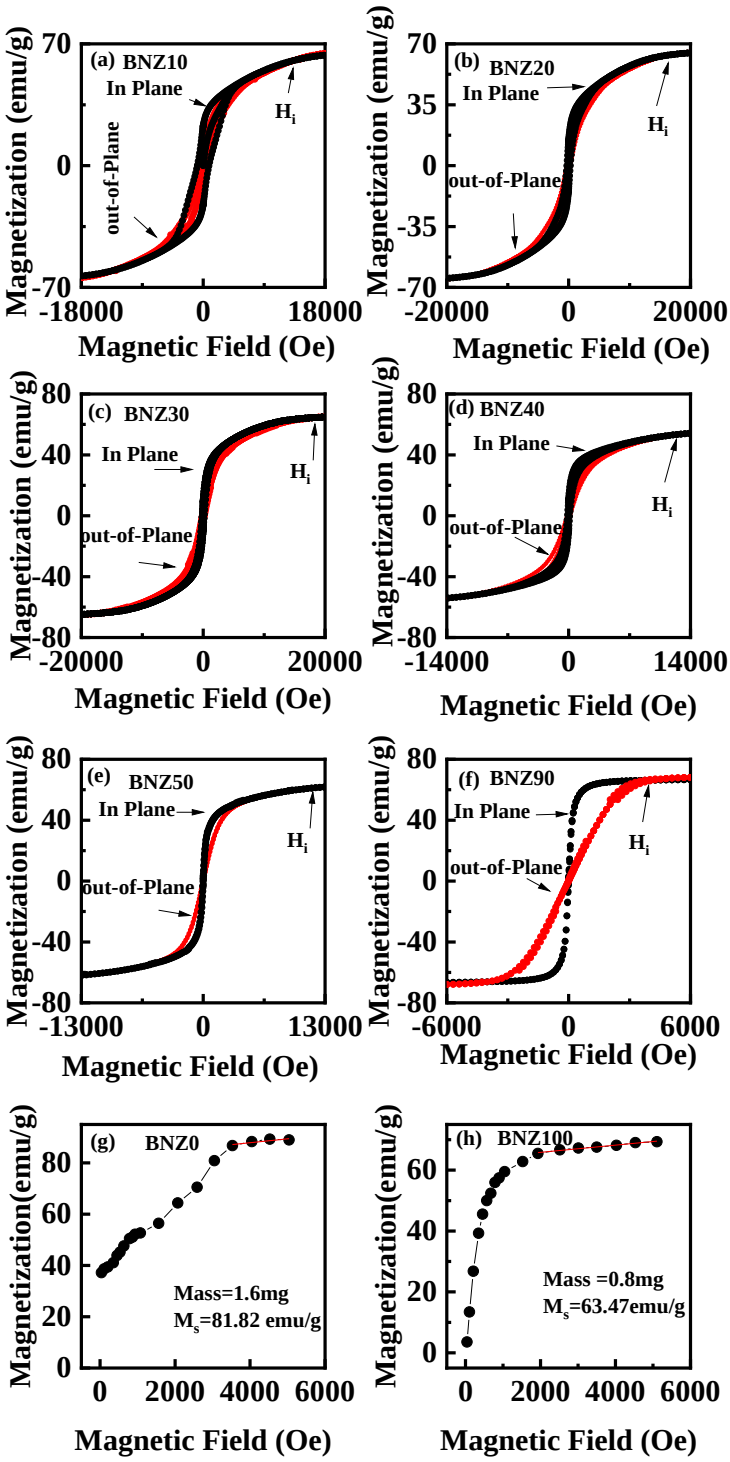


Figure S-4. In-plane *(black) and out-of-plane (red) magnetic hysteresis loops of BNZx (x=10,20,30,40,50,90) composites and (g) and (h)shows M vs H of BNZ0 (PureBaM) and BNZ100 (Pure NZFO).*

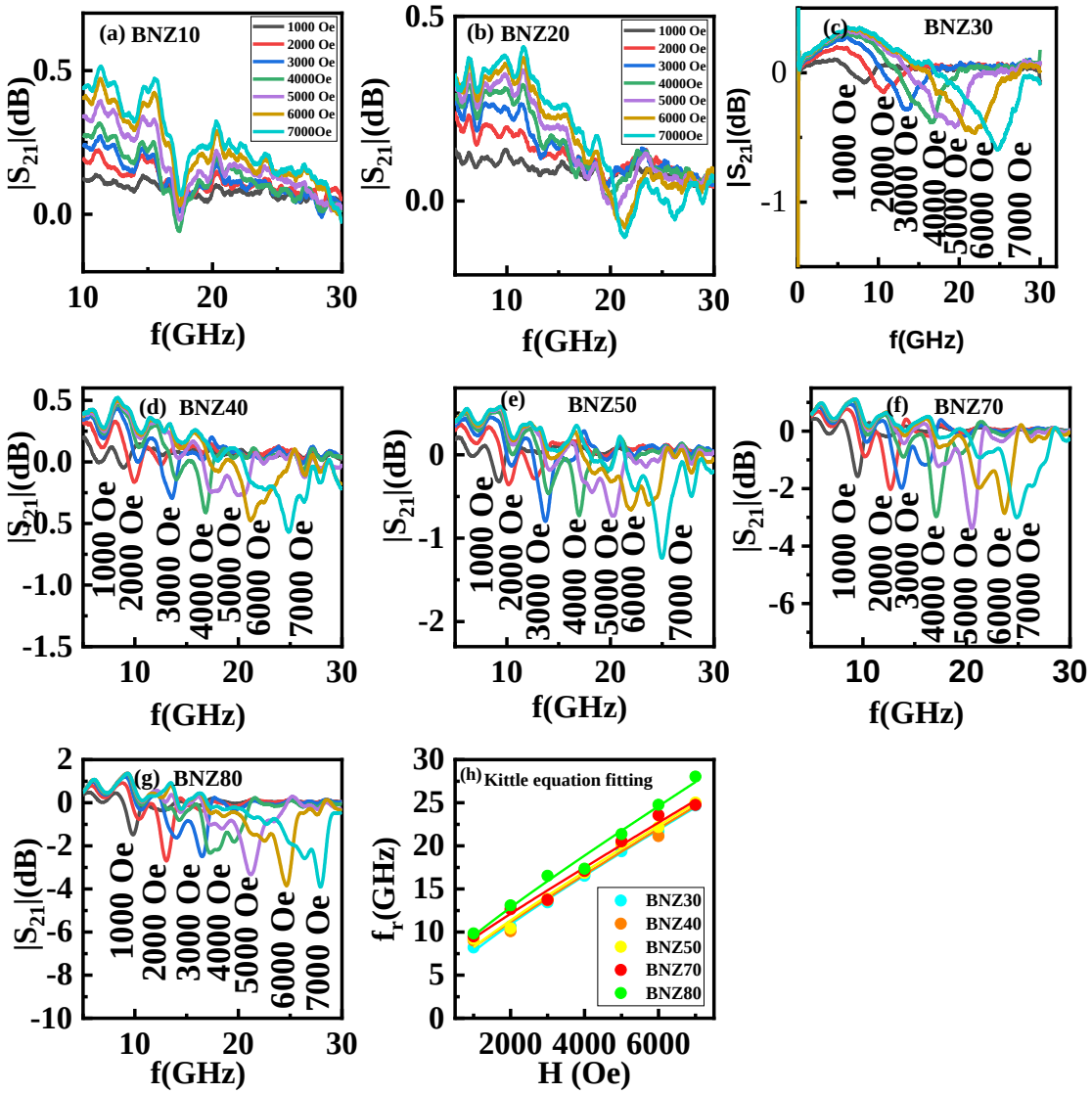


Figure S-5. (a,b,c,d,e,f,g,) Represents Profiles of S_{21} vs f in BNZx (x=10,20,30,40,50,70 and 80) composites for in-plane static magnetic fields, and (h) represents fitting of the FMR data on f_r vs H to the Kittel equation.

Table S-3: Demagnetization factors for BNZ composites

Samples	Nx	Ny	Nz
BNZ10	0.07292	0.13319	0.79389
BNZ20	0.13489	0.24346	0.62165
BNZ30	0.14955	0.17921	0.67124
BNZ40	0.10743	0.20030	0.69227
BNZ50	0.09898	0.15095	0.75007
BNZ60	0.08994	0.17531	0.73475
BNZ70	0.10758	0.21703	0.67539
BNZ80	0.07044	0.14609	0.78348
BNZ90	0.09159	0.17791	0.73050

Table S-4: Fitting parameters for FMR and magnetic parameters for BNZx composities

Samples	**γ (MHz/Oe)**	**$4\pi M_{eff}$ (kG)**	**$4\pi M$ (kG)**	**H_A(kOe) (FMR)**	**H_i (kOe) (from M vs H)**	**H_A(kOe) (M vs H)**
BNZ10	–	–	3.19	-	13.35	9.07
BNZ20	–	–	3.18	-	16.29	12.00
BNZ30	2.49	11.81	3.47	8.34	17.86	13.62
BNZ40	2.57	8.23	3.08	5.14	12.44	8.79
BNZ50	2.51	9.55	3.66	5.88	11.56	7.39
BNZ60	2.50	9.85	3.83	6.01	7.29	3.15
BNZ70	2.50	9.87	3.97	5.90	4.26	0.14
BNZ80	2.69	9.06	4.25	4.81	3.75	-0.48
BNZ90	2.69	10.23	4.51	5.72	4.01	-0.46

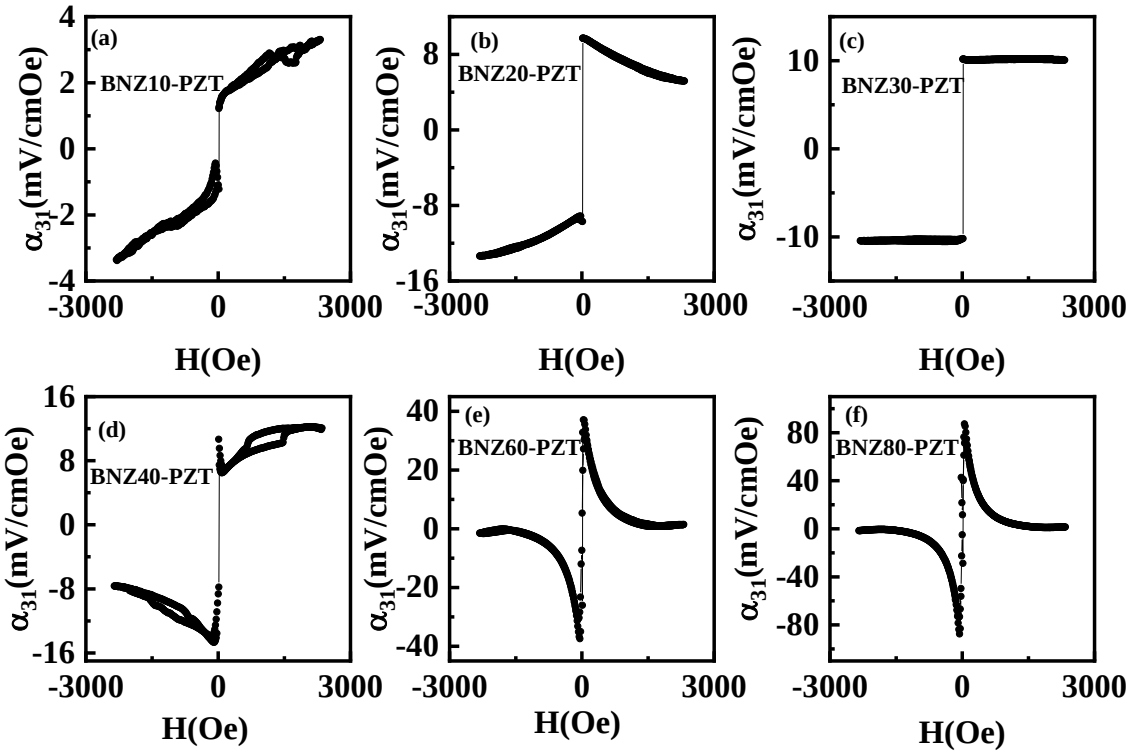


Figure S-6. α_{31} *vs H for the BNZx (x=10,20,30,40,60, and 80)PZT bilayers.*

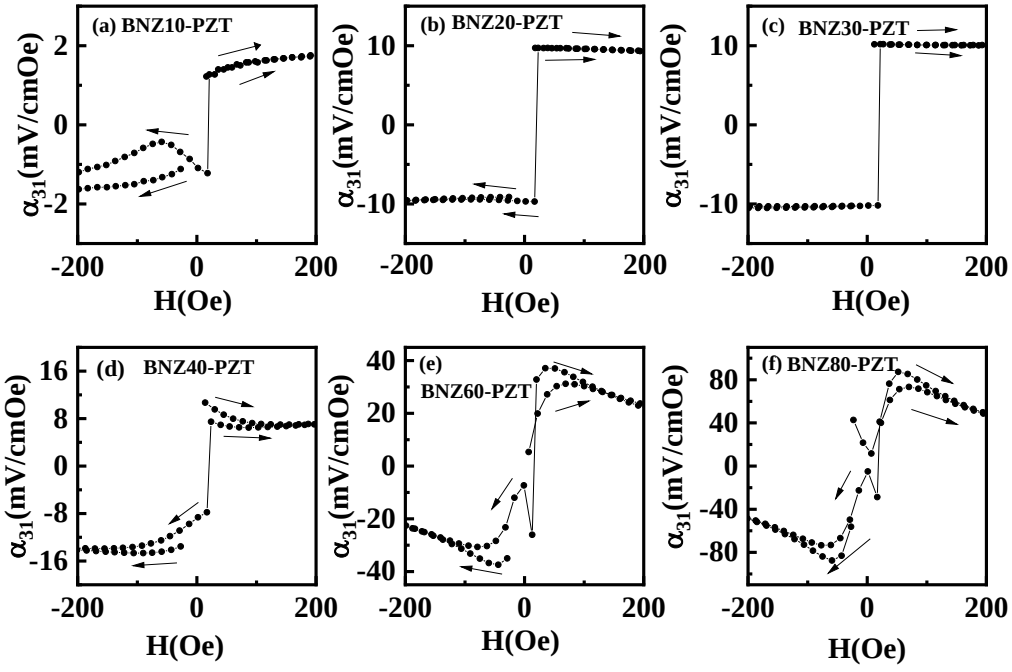


Figure S-7. Zero-bias region of α_{31} *vs H for the BNZx (x=10,20,30,40,60, and 80)PZT bilayers. The arrows represent the increasing and decreasing magnitude of H variation.*

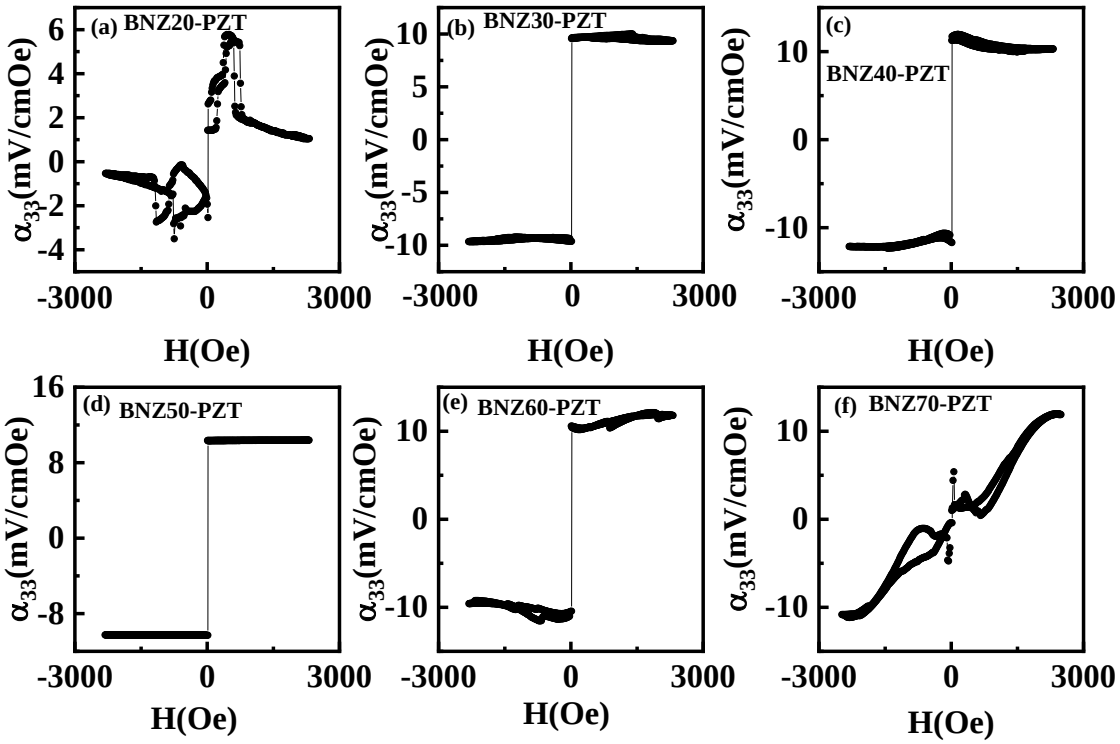


Figure S-8. α_{33} *vs H for the BNZx (x=20,30,40,50,60, and 70)PZT bilayers.*

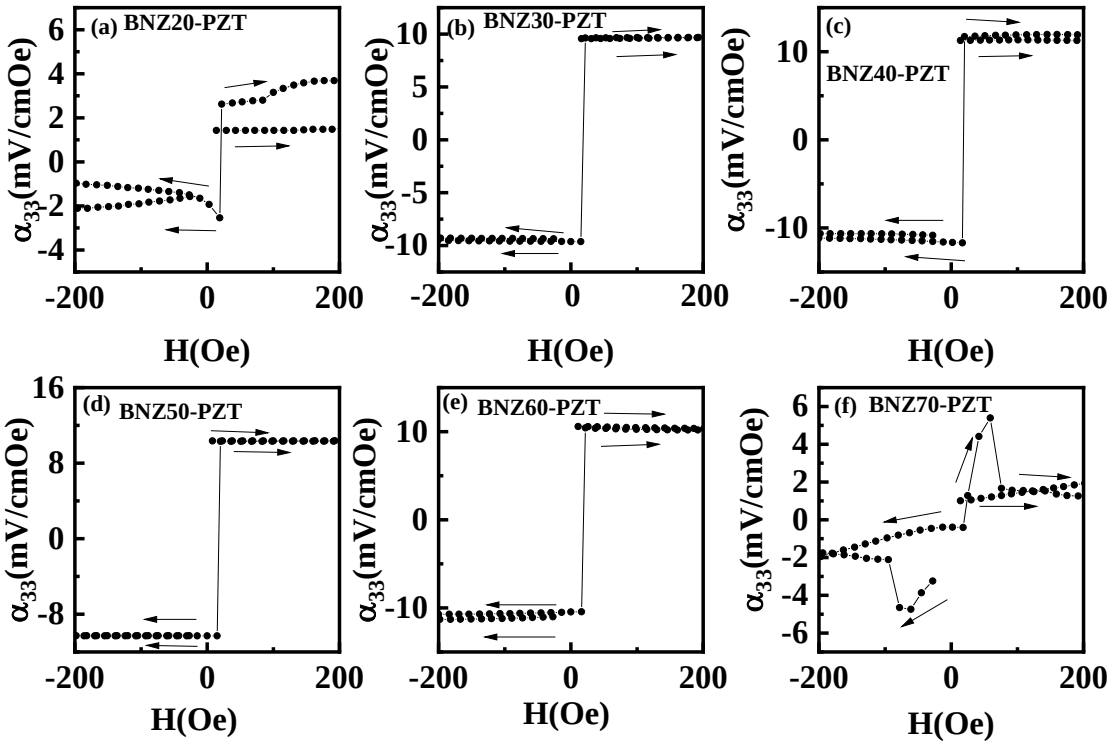


Figure S-9. Zero bias region of α_{33} vs H for the BNZx (x=20,30,40,50,60, and 70)PZT bilayers. The arrows represent the increasing and decreasing magnitude of H variation.

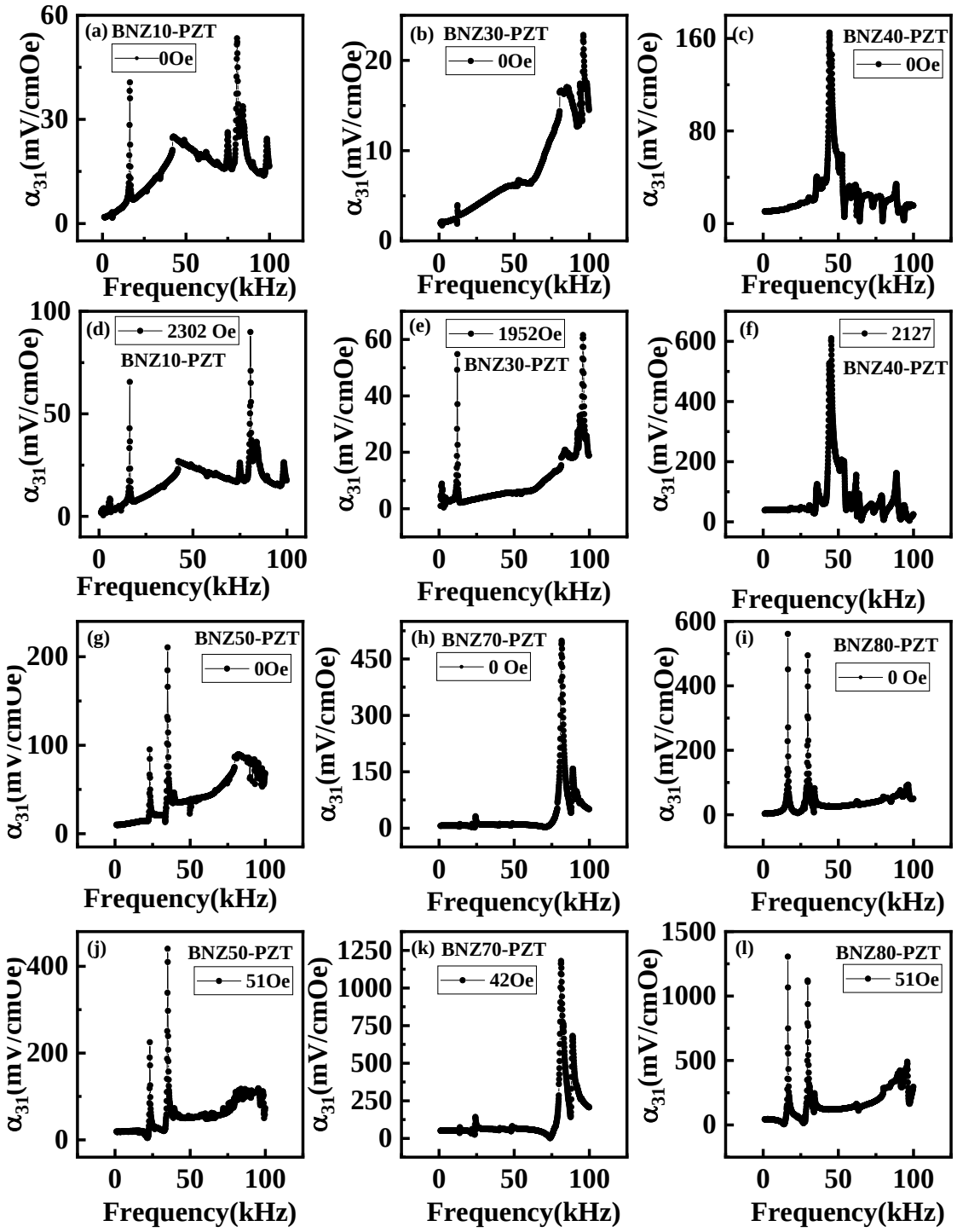


Figure S-10. Frequency dependence of ME coefficient α_{31} for BNZxPZT (x=10, 30, 40, 50, 70, and 80)PZT bilayers.